Continuous-flow dielectrophoretic trapping and patterning of colloidal particles in a ratchet microchannel

2014 J. Micromech. Microeng. 24 075007

(http://iopscience.iop.org/0960-1317/24/7/075007)

IOP Publishing Journal of Micromechanics and Microengineering
J. Micromech. Microeng. **24** (2014) 075007 (6pp) doi:10.1088/0960-1317/24/7/075007

Continuous-flow dielectrophoretic trapping and patterning of colloidal particles in a ratchet microchannel

A Kale, X Lu, S Patel and X Xuan

Department of Mechanical Engineering, Clemson University, Clemson, SC 29634-0921, USA

E-mail: xcxuan@clemson.edu

Received 20 March 2014, revised 23 April 2014
Accepted for publication 2 May 2014
Published 29 May 2014

Abstract

Trapping and concentrating particles in a continuous flow is critical for their detection and analysis as well as removal in many fields. A variety of electrical and non-electrical forces have been demonstrated to continuously capture and enrich particles in microfluidic devices. This work presents an experimental study of the development of particle trapping in an asymmetric ratchet microchannel under dc-biased ac electric fields. The dc/ac dielectrophoretic accumulation of particles in the first pair of ratchets and the dc electrokinetic shifting of particles into the second and subsequent ratchets are studied, which are found to depend on the particle moving direction with respect to the asymmetric ratchets. The dielectrophoretically trapped particles are eventually patterned into triangular zones in all but the first pair of ratchets for both the forward and backward motions. This developing process of particle trapping can be qualitatively simulated by modifying the channel geometry in the computational domain to mimic the particle chains/clusters formed in the ratchets.

Keywords: microfluidics, electrokinetics, dielectrophoresis, trapping, concentration, patterning

(Some figures may appear in colour only in the online journal)

1. Introduction

Trapping and concentrating particles (both synthetic and biological) in a continuous flow is critical for their detection and analysis as well as removal in many fields such as environmental monitoring, food safely and water quality control [1, 2]. So far numerous techniques have been developed to enrich particles in microfluidic devices [3], among which contactless methods are often preferred over surface contact methods due to their reversible and flexible trapping [4]. A variety of non-electrical forces have been demonstrated to remotely capture and accumulate particles from continuous flows [1–3], including acoustic [5–7], magnetic [8–11], optical [12–14] fields, etc. Electric field-driven contactless concentration of particles has been implemented primarily by the use of dielectrophoresis (DEP [15–17]), which is the particle motion induced by a non-uniform electric field. Traditionally, electric field gradients are created by an array of in-channel microelectrodes, where particles can be accumulated either onto the electrode tips (i.e. positive DEP) or in between the electrodes (i.e. negative DEP) by tuning the frequency for ac electric fields [18–21].

Alternatively, DEP can also be induced around insulating structures that are fabricated inside a microchannel [22, 23]. This insulator-based DEP (i.e. iDEP) technique allows electrodes to be placed into the end-channel reservoirs, which offers advantages over the traditional electrode-based DEP (i.e. eDEP) that involves complexities in microelectrode fabrications [24–26]. DC electric fields are often used in this technique, which enables a continuous-flow dielectrophoretic manipulation of particles via the electrokinetic flow and hence eliminates the hydrodynamic pumping of the particle suspension that is required in the eDEP technique. Recently dc-biased ac electric fields have been increasingly used in iDEP for the purpose of achieving an independent control of the dc electrokinetic flow and the ac/dc dielectrophoretic motion

[24–26]. The use of iDEP for particle trapping and concentration has been demonstrated in microchannels with either an array of posts of various shapes that span the entire channel depth [27–31] or one to multiple hurdles of different geometries that attach to the channel walls [32–41]. However, these previous studies have mainly focused on whether particles can be trapped and concentrated by iDEP. Little has so far been known on how the particles are captured and subsequently enriched by the in-channel posts or hurdles. The present work attempts to answer these questions through particle experiment and simulation in a microchannel with multiple pairs of asymmetric ratchets under the application of dc-biased ac electric fields. The dielectrophoretic trapping, concentration, and patterning of colloidal particles in the ratchets are studied with both a forward motion and a backward motion with respect to the asymmetric ratchets.

2. Experiment

A picture of our experimentally used ratchet microchannel is shown in figure 1. The channel was fabricated in polydimethylsiloxane (PDMS) using the well-established method of soft lithography, the details of which are explained in our previous paper [42]. It measures 8 mm long, 500 μm wide and 25 μm deep, consisting of two arrays of 20 connected triangular ratchets along its sidewalls. As indicated in the inset of figure 1, each ratchet is 250 μm long and 200 μm wide, thereby constricting the microchannel to a smallest width of 100 μm. Further, each ratchet has a surface oriented normal to the centerline of the microchannel and the other surface is inclined to the same. According to the orientation of the ratchets with respect to the particle moving direction, which is along with the electric field in our experiments, we define forward and backward motions as follows. The particle moving direction (indicated by the block arrow in the inset of figure 1) along which the inclined surface of each ratchet follows its normal surface is named as the forward motion. Similarly, the direction along which the inclined surface precedes the normal surface is named as the backward motion.

Experiments were conducted using 1 mM phosphate buffer as the suspending fluid, whose low electric conductivity can help minimizing the Joule heating effects in the ratchet region [36, 43–45]. Polystyrene particles of 10 μm in diameter were re-suspended in the buffer at a concentration of 10^6–10^7 particles/ml. To prepare the particle suspension, 0.1% of Tween 20 (Sigma Aldrich) was also added for avoiding the sticking of particles to the wall and minimizing inter-particle interactions. Prior to experiment, the liquid levels in the end-channel reservoirs were balanced to eliminate pressure driven flow effects. Platinum electrodes of 0.5 mm diameter were introduced in the two reservoirs and a power supply coupled with a function generator was used to apply dc-biased ac voltages across the channel. The experiments were conducted at a fixed dc voltage of 100 V while the ac voltage was varied to obtain stable trapping of particles in the ratchets of the microchannel. The dc voltage was selected

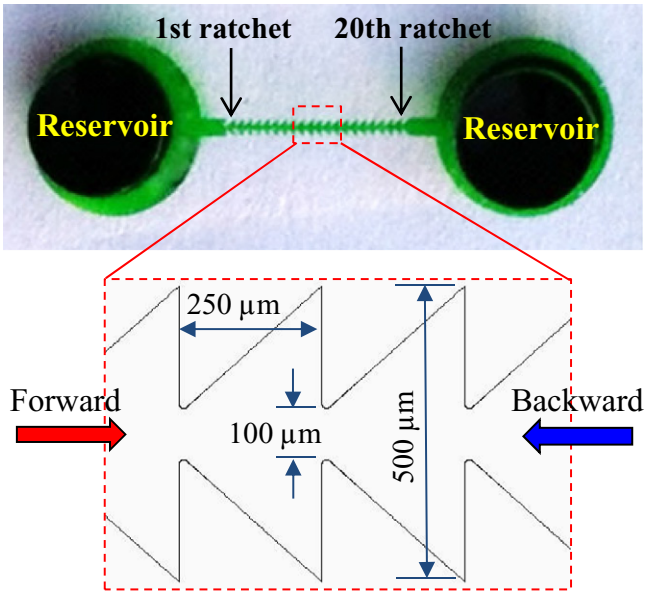

Figure 1. Picture of the ratchet microchannel (filled with green dye for visual clarity) used in experiment. The inset indicates the dimensions of each ratchet and also the specifications of the defined forward and backward motions in the text. The ratchets are numbered from 1st to 20th along the direction of the forward motion.

for obtaining a decent electrokinetic transport wherein particles can be dielectrophoretically trapped without causing significant Joule heating effects [36, 46]. The polarity of the dc voltage was switched to control the particle moving direction. The frequency of the ac voltages was maintained at 1 kHz, which, readily accessible to regular high-voltage amplifiers, was found to produce an effective particle trapping via negative DEP without noticeable particle oscillations due to ac electrokinetic flows [47]. Particle motion was visualized using an inverted microscope imaging system (Nikon Eclipse TE2000U, Nikon Instruments). The captured digital images were processed using the Nikon imaging software (NIS-Elements AR 2.30).

3. Theory

3.1. Analysis of dielectrophoretic particle trapping in a ratchet microchannel

Owing to their insulating nature, the ratchets in the microchannel create electric field gradients around them. The induced DEP, which is negative for colloidal particles suspended in a more conductive buffer [42], directs particles towards the lower electric field region i.e. away from the tip of each ratchet in all directions of the horizontal plane. Therefore, as seen from figure 2, the stream-wise component of this motion, U_{DEP_s}, is against the electrokinetic velocity, U_{EK}, and can overcome the latter yield particle trapping. To understand the effects of the particle moving direction i.e. forward or backward motion as specified in figure 1, we introduce below via scaling analysis a dimensionless number, $\tau = U_{DEP\_s}/U_{EK}$ for a qualitative interpretation of the factors

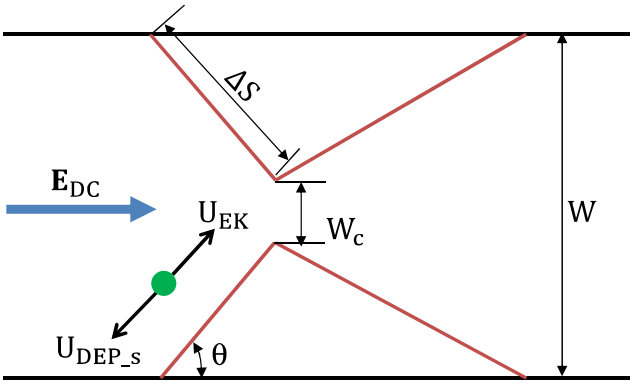

Figure 2. Schematic diagram for the theoretical analysis of dielectrophoretic particle trapping in a generalized ratchet microchannel.

that may affect the particle trapping in an asymmetric ratchet microchannel [42, 48],

$$\tau = \frac{\mu_{DEP}(1+\alpha^2)\nabla_s E_{DC}^2}{\mu_{EK} E_{DC}} = 2(1+\alpha^2)\frac{\mu_{DEP}}{\mu_{EK}}\nabla_s E_{DC} \quad (1)$$

In this equation, μ_{DEP} is the dielectrophoretic mobility of the particle, $\alpha = E_{AC}/E_{DC}$ is the ac to dc electric field ratio, ∇_s is the stream-wise gradient, and μ_{EK} is the elect rokinetic particle mobility. Consider a microchannel of width W, and a ratchet pair constricting it to a minimum width of W_c. Assume that the front surface of the ratchet has a length of ΔS and makes an angle of θ with respect to the microchannel; see the labeled dimensions in figure 2. For a channel of a uniform depth, the electric field gradients are two-dimensional in the horizontal plane only, where the dc electric field in the constriction, E_{DC_c} is given by

$$E_{DC\_c} \sim E_{DC}\frac{W}{W_c} = rE_{DC} \quad (2)$$

with $r = W/W_c$ being the width ratio of the microchannel to the constriction. Hence, the stream-wise gradient of the electric field can be scaled as,

$$\nabla_s E_{DC} \sim \frac{E_{DC\_c} - E_{DC}}{\Delta S} = \frac{E_{DC}(r-1)}{\frac{W_c(r-1)}{2\sin\theta}} = \frac{2E_{DC}}{W} r\sin\theta \quad (3)$$

Substituting equation (3) into equation (1) leads to,

$$\tau \sim (1+\alpha^2)\frac{\mu_{DEP}}{\mu_{EK}}\frac{E_{DC}}{W} r\sin\theta \quad (4)$$

For a fixed channel/constriction width ratio, r, the trapping number (note that $\tau \geq 1$ indicates a trapping) increases with the inclination angle, θ, of the ratchet (see figure 2). Therefore, the forward motion, where $\theta = \pi/2$, yields a larger trapping number than the backward motion, $\theta = \pi/4$, in the ratchet microchannel displayed in figure 1. Since μ_{DEP} is a second-order function of particle diameter [*cf*, equation (6)], larger particles experience a greater value of τ in the ratchets than smaller ones at the same working conditions, indicating an easier and more efficient trapping of the former.

3.2. Numerical modeling

To simulate the dielectrophoretic particle trapping and concentration in the ratchet microchannel, we developed a Lagrangian tracking method-based numerical model in COMSOL Multiphysics 4.3a. The details of this model are referred to our earlier papers [42, 47]. Briefly, the instantaneous particle velocity, U_P, is written as the vector sum of the dc electrokinetic velocity and the dc/ac dielectrophoretic velocity, i.e.

$$U_P = \mu_{EK} E_{DC} + \lambda\mu_{DEP}(1+\alpha^2)\nabla E_{DC}^2 \quad (5)$$

$$\mu_{DEP} = -\frac{d^2\varepsilon}{24\eta} \quad (6)$$

Here λ is the correction factor of the DEP velocity to account for the perturbation of the electric and flow field distributions due to the presence of the particle and the channel walls, d is the particle diameter, and ε and η are the permittivity and dynamic viscosity of the suspending fluid, respectively. Note that the Clausius-Mosotti factor has been assumed to be –0.5 in equation (6) because the particle electric conductivity is negligible compared to that of the fluid [42]. The numerical simulations of the experiments were generated using the electrostatics interface (for electric potential distribution) and the particle tracing function (for particle trajectory) in COMSOL. The electrokinetic particle mobility, μ_{EK}, was measured directly from the particle motion in the straight section of the ratchet microchannel, which was found to be 2.6×10^{-8} m^2/(V·s). The dielectrophoretic particle mobility, μ_{DEP}, was calculated from equation (6) with the fluid permittivity and viscosity being taken as 7.11×10^{10} F/m and 0.001 Pa·s, respectively.

4. Results and discussion

Figure 3 illustrates the experimentally obtained images and numerically predicted trajectories of 10 μm particles when they are initially trapped (5 s after the trapping started, and thus not yet significantly concentrated) by iDEP before the first pair of ratchets with the forward (a) and backward (b) motions, respectively. The applied dc voltage across the channel is 100 V in both cases while the imposed ac voltages, each of which is the minimum to initiate a dielectrophoretic trapping, are 650 V and 850 V for the forward and backward motions, respectively. Note that both threshold values were determined by gradually increasing the ac voltages till particles started being trapped. The smaller ac to dc voltage (and hence field) ratio in the former case is consistent with the scaling analysis of the defined trapping number, i.e. τ in equation (4), which increases with the angle of the ratchet with respect to the microchannel, i.e. θ in figure 2. The correction factor, λ, for particle DEP in equation (5) in the numerical model was set to 0.5 in both the forward and backward motions, which is consistent with the values used in our previous studies [42, 49, 50]. The obtained particle trajectories from the simulation

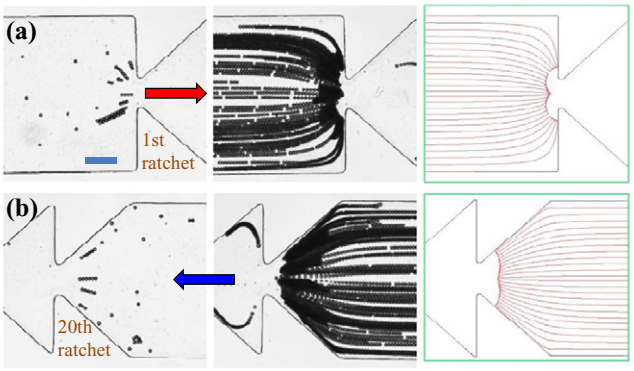

Figure 3. Comparison of experimentally obtained images (snapshot in the left column and composite in the middle column) and numerically predicted trajectories (right column) of 10 μm particles that are dielectrophoretically trapped before the first pair of ratchets at the early stage (5 s after the particle trapping started in each case): (*a*) forward motion under the application of 100 V dc-biased 650 V ac voltage; (*b*) backward motion under the 100 V dc-biased 850 V ac voltage. The block arrows indicate particle moving directions (see also the definitions in figure 1). The scale bar on the left-most image of (*a*) represents 100 μm.

(right column) agree reasonably with the composite particle image from the experiment (middle column) in each case as demonstrated in figure 3. The snapshot images in the left column indicate that at the early stage of dielectrophoretic trapping, particles form multiple short chains which tend to be scattered before the first pair of ratchets in both the forward and backward motions.

With particles being continuously trapped, more short chains are formed in the forward motion, which then interact with each other leading to the formation of particle clusters. As demonstrated in the snapshot image in figure 4(*a1*) (top), the clusters are patterned against the front edges of the first pair of ratchets and inclined to drift away from the tips towards the rear parts of the ratchets. In contrast, longer chains are formed with more particles getting trapped in the backward motion, which extend upstream and seem to be evenly distributed at the entrance of the first pair of ratchets. This dissimilar style of particle concentration is illustrated by the image in figure 4(*b1*) (top). When the number of trapped particles goes beyond a certain value, some particles (either individual or in a chain) can escape from the first pair of ratchets and travel into the second pair where they get trapped again by DEP. This trend occurs for both the forward and backward motions in the ratchet microchannel. It is because the non-conducting particles that are concentrated before the first pair of ratchets tend to reduce the local electric field gradients and hence DEP, which is qualitatively simulated by the particle trajectories in figures 4(*a1*), (*b1*) (bottom). In this revised model, the impact of the formed dielectric particle chains/clusters in the first pair of ratchets was considered by modifying the computational geometry, which has been highlighted by the filled circles on the numerical images. Specifically, those highlighted boxes in figures 4(*a1*), (*b1*) (bottom) were treated as insulators in the numerical model, through which electric field lines were unable to penetrate.

The enrichment of particles trapped by the second pair of ratchets follow a similar style to that in the first pair for the

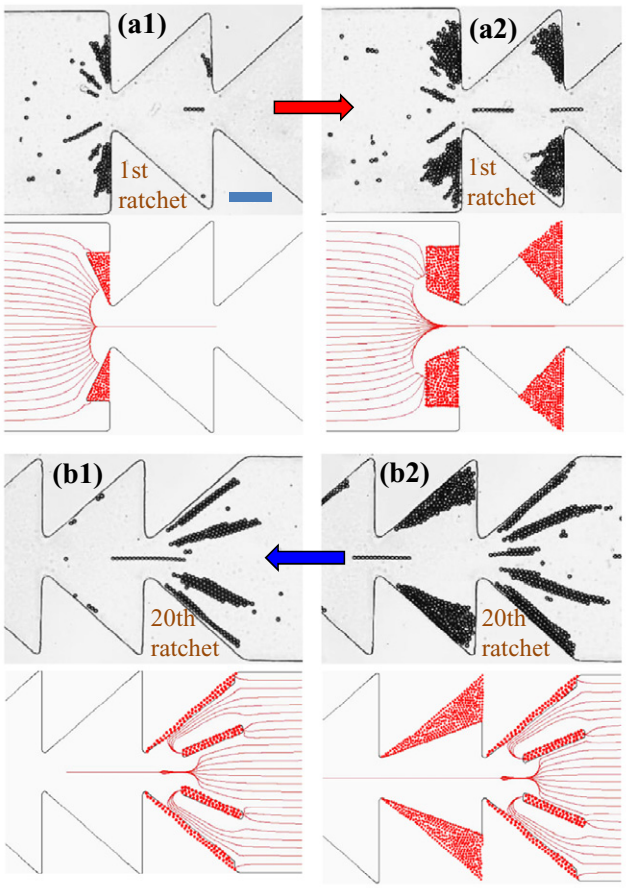

Figure 4. Development of the dielectrophoretic trapping and concentration of 10 μm particles in the first pair of ratchets (*a1*), (*b1*) and subsequently in the second pair of ratchets (*a2*), (*b2*): (*a1*), (*a2*) forward motion under the application of 100 V dc-biased 650 V ac voltage; (*b1*), (*b2*) backward motions under the 100 V dc-biased 850 V ac voltage. The top and bottom images of each panel show the experimentally recorded snapshot image and numerically predicted particle trajectories, respectively. The formed particle chains/clusters in experiments are mimicked by modifying the channel geometry in simulations (see the parts highlighted by filled circles on the numerical images). The block arrows indicate the particle moving directions. The scale bar on the experimental image of (*a1*) represents 100 μm.

forward motion as demonstrated from the image in figure 4(*a2*) (top). In contrast, the trapped particles in the backward motion are all pushed towards the front edges of the second pair of ratchets and patterned along nearly the entire length of these two surfaces, which as seen from the image in figure 4(*b2*) (top), is different from the particle behavior in the first pair. In both cases, when the trapped particles keep building up, some of the particles can no longer be trapped by the second pair of ratchets and will move into the third pair. This is still the consequence of the weakened DEP and is numerically predicted in figures 4(*a2*), (*b2*) (bottom). Such a trend of particle escaping, trapping, and patterning from one pair of ratchets to the other is repeated till the last pair in the ratchet microchannel for both the forward and backward motions.

Figure 5(*a*) shows the snapshot images of particle patterning in only the first four pairs of ratchets at the late stage of dielectrophoretic trapping (5 min after the trapping

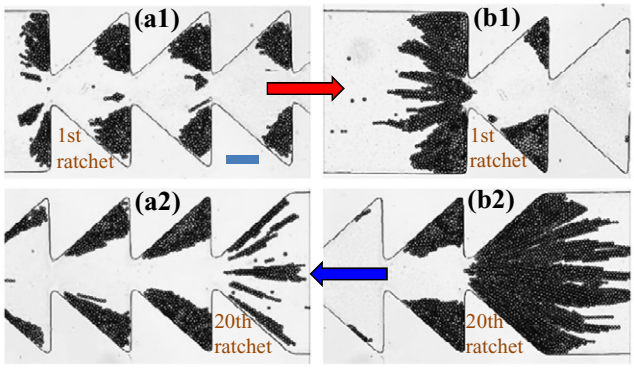

Figure 5. Snapshot images illustrating the dielectrophoretic patterning of 10 μm particles in the ratchet microchannel at the late stage of dielectrophoretic trapping (5 min after the trapping started): (*a1*) forward motion under 100 V dc/650 V ac (threshold ac voltage for trapping); (*a2*) backward motion under 100 V dc/850 V ac (threshold ac voltage for trapping); (*b1*) forward motion under 100 V dc/1050 V ac; (*b2*) backward motion under 100 V dc/1250 V ac. The block arrows indicate the particle moving directions. The scale bar on the image in (a1) represents 100 μm.

started) in the forward (top) and backward (bottom) motions, respectively. It is, however, important to note that particles are trapped equally well in the rest of the ratchets in both cases (images not shown). Moreover, the shapes of the particle trapping zone remain unvaried in all but the first pair of ratchets for each case. Hence, the total number of particles that can be trapped and accumulated in the ratchet microchannel, i.e. the trapping capacity, is approximately a linear function of the number of ratchet pairs. Only after sufficient number of particles were trapped and patterned throughout the channel have we observed the escaping of particles from the last pair of ratchets in both the forward and backward motions. In other words, the particle trapping efficiency is 100% in this ratchet microchannel before the maximum trapping capacity is reached. We can increase the particle trapping capacity by the use of higher electric fields for an enhanced DEP, which, however, may cause a blockage of the microchannel due to the over-concentration of particles before the first pair of ratchets. This latter phenomenon is demonstrated by the experimentally recorded images in figure 5(*b*) for both the forward (top) and backward (bottom) motions in the ratchet microchannel. The applied dc voltage across the microchannel is still fixed at 100 V while the ac voltage is 400 V higher than the threshold value of dielectrophoretic trapping (see figure 3) in both cases.

5. Conclusions

We have studied the development of continuous-flow dielectrophoretic particle trapping in a microchannel with multiple pairs of asymmetric ratchets under dc-biased ac electric fields. The threshold ac voltage for particle trapping at a fixed dc voltage is found lower in the forward motion than in the backward motion, which is consistent with the theoretical analysis of a dimensionless trapping number. The dielectrophoretic accumulation of particles in the first pair of ratchets and the electrokinetic shifting of particles into the second and subsequent ratchets are observed, which differ between the forward and backward motions. This process can be qualitatively simulated by modifying the channel geometry in the simulation to mimic the dielectric particle chains/clusters formed inside the ratchets. Eventually triangular trapping zones are formed in all but the first pair of ratchets for both the forward and backward motions. The particle trapping capacity of a ratchet microchannel is found to increase with the number of ratchet pairs and can also be enhanced by increasing the ac electric field. The latter, however, has been found to possibly cause channel blockage before the first pair of ratchets by the over-concentrated particles.

Acknowledgments

This work was partially supported by NSF under Grant No. CBET-0853873.

References

[1] Pratt E D, Huang C, Hawkins B G, Gleghorn J P and Kirby B J 2011 *Chem. Eng. Sci.* **66** 1508–22
[2] Karimi A, Yazai S and Ardekani A M 2013 *Biomicrofluidics* **7** 021501
[3] Nilsson J, Evander M, Hammarstrom B and Laurell T 2009 *Anal. Chim. Acta* **649** 141–57
[4] Johann R M 2006 *Anal. Bioanal. Chem.* **385** 408–12
[5] Shi J, Mao X, Ahmed D, Colletti A and Huang T J 2008 *Lab Chip* **8** 221–3
[6] Hammarstrom B, Evander M, Barbeau H, Bruzelius M, Larsson J, Laurell T and Nilsson J 2010 *Lab Chip* **10** 2251–7
[7] Chen Y, Li S, Gu Y, Li P, Ding X, McCoy J P, Levine S J, Wang L and Huang T J 2014 *Lab Chip* **14** 924–30
[8] Peyman S A, Kwan E Y, Margarson O, Iles A and Pamme N 2009 *J. Chromatogr.* A **1216** 9055–62
[9] Zeng J, Chen C, Vedantam P, Tzeng T and Xuan X 2013 *Microfluidics Nanofluidics* **15** 49–55
[10] Tarn M D, Peyman S A and Pamme N 2013 *RSC Adv.* **3** 7209–14
[11] Wilbanks J J, Kiessling G, Zeng J, Zhang C and Xuan X 2014 *J. Appl. Phys.* **115** 044907
[12] Kumar A, Kwon J S, Williams S J, Green N G, Yip N K and Wereley S T 2010 *Langmuir* **26** 5262–72
[13] Williams S J, Kumar A, Green N G and Wereley S T 2010 *J. Micromech. Microeng.* **20** 015022
[14] Zhang Y, Lei H, Li Y and Li B 2012 *Lab Chip* **12** 1302–8
[15] Lapizco-Encinas B H and Rito-Palmomares M 2007 *Electrophoresis* **28** 4521–38
[16] Shafiee H, Caldwell J L, Sano M B and Davalos R D 2009 *Biomed. Microdevices* **11** 997–1006
[17] Jesús-Pérez N M and Lapizco-Encinas B H 2011 *Electrophoresis* **32** 2331–57
[18] Gascoyne P R C and Vykoukal J 2002 *Electrophoresis* **23** 1973–83
[19] Cetin B and Li D 2009 *Electrophoresis* **30** 3124–33
[20] Hughes M P 2002 *Electrophoresis* **23** 2569–82
[21] Pethig R 2010 *Biomicrofluidics* **4** 1–35
[22] Chou C F, Tegenfeldt J O, Bakajin O, Chan S S, Cox E C, Darnton N, Duke T and Austin R H 2002 *Biophys. J.* **83** 2170–9
[23] Cummings E B and Singh A K 2003 *Anal. Chem.* **75** 4724–31

[24] Srivastava S K, Gencoglu A and Minerick A R 2010 *Anal. Bioanal. Chem.* **399** 301–21
[25] Regtmeier J, Eichhorn R, Viefhues M, Bogunovic L and Anselmetti D 2011 *Electrophoresis* **32** 2253–73
[26] Li M, Li W H, Zhang J, Alici G and Wen W 2014 *J. Phys.* D: *Appl. Phys.* **47** 063001
[27] Lapizco-Encinas B H, Simmons B A, Cummings E B and Fintschenko Y 2004 *Electrophoresis* **25** 1695–704
[28] Ozuna-Chacón S, Lapizco-Encinas B H, Rito-Palomares M, Martínez-Chapa S O and Reyes-Betanzo C 2008 *Electrophoresis* **29** 3115–22
[29] Sabounchi P, Morales A M, Ponce P, Lee L P, Simmons B A and Davalos R V 2008 *Biomed. Microdevices* **10** 661–70
[30] Sano M B, Gallo-Villanueva R C, Lapizco-Encinas B H and Davalos R V 2013 *Microfluidics Nanofluidics* **15** 599–609
[31] Gallo-Villanueva R C, Sano M B, Lapizco-Encinas B H and Davalos R V 2014 *Electrophoresis* **35** 352–61
[32] Hawkins B G, Smith A E, Syed Y A and Kirby B J 2007 *Anal. Chem.* **79** 7291–300
[33] Church C, Zhu J, Huang G, Tzeng T and Xuan X 2010 *Biomicrofluidics* **4** 044101
[34] Lewpiriyawong N, Yang C and Lam Y C 2012 *Microfluidics Nanofluidics* **12** 723–33
[35] Braff W A, Pignier A and Buie C R 2012 *Lab Chip* **12** 1327–31
[36] Zhu J, Sridharan S, Hu G and Xuan X 2012 *J. Micromech. Microeng.* **22** 075011
[37] Chaurey V, Rohani A, Su Y H, Liao K T and Chou C F 2013 *Electrophoresis* **34** 1097–104
[38] Pysher M D and Hayes M A 2007 *Anal. Chem.* **79** 4552–7
[39] Chen K P, Pacheco J R, Hayes M A and Staton S J R 2009 *Electrophoresis* **30** 1441–8
[40] Staton S J R, Chen K P, Taylor T J, Pacheco J R and Hayes M A 2010 *Electrophoresis* **31** 3634–41
[41] Jones P V, Staton S J R and Hayes M A 2011 *Anal. Bioanal. Chem.* **401** 2103–11
[42] Zhu J and Xuan X 2009 *Electrophoresis* **30** 2668–75
[43] Hawkins B G and Kirby B J 2010 *Electrophoresis* **31** 3622–33
[44] Sridharan S, Zhu J, Hu G and Xuan X 2011 *Electrophoresis* **32** 2274–81
[45] Chaurey V, Polanco V, Chou C F and Swami N S 2012 *Biomicrofluidics* **6** 012806
[46] Kale A, Patel S, Hu G and Xuan X 2013 *Electrophoresis* **34** 674–83
[47] Patel S, Qian S and Xuan X 2013 *Electrophoresis* **34** 961–8
[48] Kale A, Patel S, Qian S, Hu D and Xuan X 2014 *Electrophoresis* **35** 721–7
[49] Kang K, Xuan X, Kang Y and Li D 2006 *J. Appl. Phys.* **99** 064702
[50] Zhu J, Tzeng T, Hu G and Xuan X 2009 *Microfluidics Nanofluidics* **7** 751–6